Finite steady-state current defies non-Hermitian many-body localization

Pietro Brighi , Marko Ljubotina , Federico Roccati , fo and Federico Balducci , and Federico Balducci ¹Faculty of Physics, University of Vienna, Boltzmanngasse 5, 1090 Vienna, Austria ²Physics Department, TUM School of Natural Sciences, Technical University of Munich, 85748 Garching, Germany ³Munich Center for Quantum Science and Technology (MCQST), Schellingstraße 4, 80799 München, Germany ⁴Institute of Science and Technology Austria, Am Campus 1, 3400 Klosterneuburg, Austria ⁵Quantum Theory Group, Dipartimento di Fisica e Chimica Emilio Segrè, Università degli Studi di Palermo, via Archirafi 36, I-90123 Palermo, Italy ⁶Max Planck Institute for the Science of Light, 91058 Erlangen, Germany

⁷Max Planck Institute for the Physics of Complex Systems, Nöthnitzer Straße 38, 01187 Dresden, Germany

(Received 14 April 2025; revised 10 July 2025; accepted 12 September 2025; published 14 October 2025)

Non-Hermitian many-body localization (NH MBL) has emerged as a possible scenario for stable localization in open systems, as suggested by spectral indicators identifying a putative transition for finite system sizes. In this work, we shift the focus to dynamical probes, specifically the steady-state spin current, to investigate transport properties in a disordered, non-Hermitian XXZ spin chain. Through exact diagonalization for small systems and tensor-network methods for larger chains, we demonstrate that the steady-state current remains finite and decays exponentially with disorder strength, showing no evidence of a transition up to disorder values far beyond the previously claimed critical point. Our results reveal a stark discrepancy between spectral indicators, which suggest localization, and transport behavior, which indicates delocalization. This highlights the importance of dynamical observables in characterizing NH MBL and suggests that traditional spectral measures may not fully capture the physics of non-Hermitian systems. Additionally, we observe a noncommutativity of limits in system size and time, further complicating the interpretation of finite-size studies. These findings challenge the existence of NH MBL in the studied model and underscore the need for alternative approaches to understanding localization in non-Hermitian settings.

DOI: 10.1103/crwj-x7j8

Introduction. Non-Hermitian (NH) Hamiltonians are a ubiquitous tool used to capture the dissipative nature of realistic quantum systems [1]. While an NH Hamiltonian does not fully characterize the dynamics of an open quantum system, it does when postselecting on the no-jump trajectories (no-click limit) [2]. Recently, the interplay of many-body and NH physics has garnered significant interest due to the intriguing phenomena emerging in this setting. These include interaction-induced and many-body skin effect [3-5], skin solitons [6], nonlinear exceptional points [7,8], and NH manybody localization (MBL) [9].

In Hermitian MBL, the presence of disorder can suppress transport, resulting in a nonthermal insulating phase [10–16]. The absence of transport and the breakdown of ergodicity have been used interchangeably as hallmarks of many-body localization, leading to the wide use of spectral indicators to detect MBL [17–21]. In the context of open quantum systems, a large body of literature has shown that Hermitian MBL is

Published by the American Physical Society under the terms of the Creative Commons Attribution 4.0 International license. Further distribution of this work must maintain attribution to the author(s) and the published article's title, journal citation, and DOI. Open access publication funded by Max Planck Society.

destabilized by any bath with a continuous spectrum [22–34]. However, as pointed out originally in Ref. [9], localization seems to persist in the no-click limit. This paradox can be resolved in some models, where it is possible to generalize to the many-body setting the similarity transformation that maps the non-Hermitian Hamiltonian to its Hermitian counterpart [35]. While the transformation is legitimate only with open boundary conditions, in the localized phase, it is expected that the boundary conditions are irrelevant, thus enabling a mapping of the Hermitian MBL phase onto the NH MBL phase [36].

On the footsteps of the standard Hermitian case, many works have focused on the behavior of the spectra and eigenstates of NH Hamiltonians [37-44]—and sometimes on other indicators such as the singular value decomposition [45]. In non-Hermitian systems, however, dynamics lead to a unique steady state and the properties of the middle of the spectrum are less relevant than in the Hermitian case. This calls for more physically motivated probes of localization, such as the exponential suppression of transport with system size, a defining feature of (Hermitian) localization [10,11,46,47], which has rarely been investigated in the non-Hermitian setting [48].

In this work, we consider the disordered non-Hermitian XXZ chain and study the behavior of the spin current in the steady state by means of exact diagonalization (ED) for small system sizes and tensor-network methods (timeevolving block decimation, TEBD [49]) for systems of up to

^{*}Contact author: fbalducci@pks.mpg.de

N=560 spins. We find that the steady-state current is exponentially suppressed with the disorder strength in the range of parameters we investigate. Remarkably, the steady-state current does not display a nonanalyticity as a function of the disorder strength and remains finite up to values of disorder well beyond the putative critical point identified through spectral indicators at the center of the complex spectrum [9]. This points to the absence of a true phase transition for observables (i.e., expectation values of Hermitian operators), suggesting that if localization takes place, it does so at higher disorder strengths. Our work indicates that traditional spectral measures of Hermitian MBL do not necessarily translate to its NH counterpart, where the role of states in the middle of the spectrum is less central to long-time dynamical properties.

Model. We study a one-dimensional *N*-site spin chain governed by an NH Hamiltonian

$$\hat{H}_{\text{eff}} = \hat{H} - \iota \hat{\Gamma} = \hat{H} - \frac{\iota}{2} \sum_{i=1}^{N} \hat{L}_{j}^{\dagger} \hat{L}_{j}, \tag{1}$$

which describes the no-click limit of a Lindblad master equation $\dot{\rho} = -\iota[\hat{H},\rho] + \sum_j \mathcal{D}[\hat{L}_j]\rho$, where $\mathcal{D}[\hat{L}]\rho = \hat{L}\rho\hat{L}^\dagger - (\hat{L}^\dagger\hat{L}\rho + \rho\hat{L}^\dagger\hat{L})/2$ and ρ is the density matrix. The Hermitian part corresponds to the disordered XXZ chain:

$$\hat{H} = J \sum_{i=1}^{N} \left[\frac{1}{2} (\hat{S}_{j}^{-} \hat{S}_{j+1}^{+} + \hat{S}_{j}^{+} \hat{S}_{j+1}^{-}) + V \hat{S}_{j}^{z} \hat{S}_{j+1}^{z} + h_{j} \hat{S}_{j}^{z} \right], \quad (2)$$

where V is the interaction strength, h_j are i.i.d. random variables uniformly distributed over the interval [-h, h], $\hat{S}_j^{x,y,z}$ are the spin-1/2 operators acting on site j, and $\hat{S}^{\pm} = \hat{S}^x \pm \iota \hat{S}^y$. In the following, we fix the energy scale by setting J = 1. We will study the system under both open (OBCs) and periodic boundary conditions (PBCs).

The dissipative part is given by jump operators of the form $\hat{L}_j = \sqrt{\gamma} (\hat{S}_j^- + e^{i\theta} \hat{S}_{j+1}^-)$, which give rise to nonreciprocal hopping in the no-click limit [50–53]. The corresponding effective Hamiltonian is

$$\hat{H}_{\text{eff}} = \sum_{j=1}^{N} \left[\frac{1 - i\gamma e^{i\theta}}{2} \hat{S}_{j}^{+} \hat{S}_{j+1}^{-} + \frac{1 - i\gamma e^{-i\theta}}{2} \hat{S}_{j}^{-} \hat{S}_{j+1}^{+} + V \hat{S}_{j}^{z} \hat{S}_{j+1}^{z} + (h_{j} - i\gamma) \hat{S}_{j}^{z} \right] - i\gamma \frac{N}{2}.$$
 (3)

Choosing $\theta = \pm \pi/2$, the left and right hopping amplitudes become real and imbalanced. The effective Hamiltonian in Eq. (3) further acquires finite imaginary shifts proportional to the number of sites $(-\iota \gamma N/2)$ and to the global magnetization $(-\iota \gamma \sum_j \hat{S}_j^z)$, which ensure the physicality of its solutions; i.e., its eigenvalues lie in the lower part of the complex plane, and thus, the wave function norm is not exponentially amplified. Finally, mapping spins-1/2 to fermions via a Jordan-Wigner transformation, one realizes that Eq. (3) is the interacting version of the Hatano-Nelson model [35].

In the following, aligning with the existing literature on the model, we will focus on the zero magnetization sector—which effectively removes the $-\iota\gamma\sum_{j}\hat{S}_{j}^{z}$ term from the

Hamiltonian—and further drop the constant term $-\iota \gamma N/2$:

$$\hat{H}_{\text{eff}} = \sum_{j=1}^{N} \left[\frac{1-\gamma}{2} \hat{S}_{j}^{+} \hat{S}_{j+1}^{-} + \frac{1+\gamma}{2} \hat{S}_{j}^{-} \hat{S}_{j+1}^{+} + V \hat{S}_{j}^{z} \hat{S}_{j+1}^{z} + h_{j} \hat{S}_{j}^{z} \right].$$
(4)

This way, the complex spectrum becomes symmetric with respect to the real axis. We fix $\gamma = 0.1$ and V = 1.1 for all numerical simulations.

While the spectral properties of the Hamiltonian (4) have been investigated [9,37–40,42–45], the presence or absence of transport in the NH case remains an open question. Clarifying this issue in the NH case is essential, especially due to recent developments in Hermitian MBL, showing that the transition possibly takes place at much stronger disorder values than originally thought [54–60]. Crucially, in the NH setting, there exists a *steady state* coinciding with the eigenstate with the largest imaginary part of the corresponding eigenvalue [61]. Therefore, a *single eigenstate* determines transport properties at long times, in contrast with the Hermitian case, where it takes contributions from all eigenstates.

Spin transport. As both the Hermitian and non-Hermitian Hamiltonians conserve the global magnetization $\hat{S}_{\text{tot}}^z = \sum_j \hat{S}_j^z$, we characterize the system's putative localization transition through the spin current. In the Hermitian case, the Heisenberg equation of motion for a local spin obeys a continuity equation and defines the current operator: $\partial_t \hat{S}_j^z = \hat{J}_j - \hat{J}_{j-1} = (\nabla \cdot \hat{J})_j$, where ∇ is the discrete derivative, and we introduce the current operator $\hat{J}_j := \frac{1}{2}(\hat{S}_j^+ \hat{S}_{j+1}^- - \hat{S}_j^- \hat{S}_{j+1}^+)$. Including the NH terms, however, the Heisenberg equation is modified to $i\partial_t \hat{S}_j^z = \hat{S}_j^z \hat{H}_{\text{eff}} - \hat{H}_{\text{eff}}^\dagger \hat{S}_j^z$. As a consequence, the continuity equation above changes, possibly making the definition of the current invalid in the NH case.

Splitting the effective Hamiltonian (4) into Hermitian and anti-Hermitian components as in Eq. (1), one can observe that the anti-Hermitian part is proportional to the global current:

$$\hat{H}_{\text{eff}} = \hat{H} - \iota \gamma \hat{J}_{\text{tot}}, \quad \hat{J}_{\text{tot}} = \sum_{j=1}^{N} \hat{J}_{j}.$$
 (5)

It then follows that one can define a modified continuity equation for the NH case:

$$\partial_t \hat{S}_j^z = (\nabla \cdot \hat{J})_j + \gamma \{\hat{J}_{\text{tot}}, \hat{S}_j^z\}.$$
 (6)

This equation marks the difference between the NH and Hermitian cases: a nonlocal contribution to spin dynamics appears in what was a local continuity equation, as entailed by the anticommutator term. This additional term can be thought of as the source and sink induced by the local dissipation, and it is made nonlocal by the postselection procedure [62].

Before moving on, it is important to notice that the introduction of non-Hermiticity hinders the study of transport using states that are not eigenstates of the total magnetization $\hat{S}^z_{\rm tot}$ [63]. Indeed, if the initial state is an eigenstate of the magnetization, $\hat{S}^z_{\rm tot}|\psi_0\rangle = S_0|\psi_0\rangle$, then at time $t, \langle \psi(t)|\hat{S}^z_{\rm tot}|\psi(t)\rangle = S_0\langle \psi(t)|\psi(t)\rangle$, as $[\hat{H}_{\rm eff},\hat{S}^z_{\rm tot}]=0$. It is only the change in the norm of $|\psi(t)\rangle$ that causes the expectation value of $\hat{S}^z_{\rm tot}$ to change. Upon postselecting, the norm

of $|\psi(t)\rangle$ is restored to be 1, and the magnetization is truly conserved:

$$\frac{\langle \psi(t)|\hat{S}_{\text{tot}}^z|\psi(t)\rangle}{\langle \psi(t)|\psi(t)\rangle} = S_0. \tag{7}$$

However, when the initial state $|\psi_0\rangle$ is *not* an eigenstate of the magnetization, the NH dynamics does *not* conserve the weight of the wave function in each separate magnetization sector. In fact, each sector is characterized by a different minimal decay rate, and in the infinite-time limit, only one sector survives. The above reasoning also shows that experimentally relevant observables are calculated using the *right* eigenstates of NH Hamiltonians, i.e., the right steady state of $\hat{H}_{\rm eff}$ in our case [64,65].

Numerical results. We first analyze the current in eigenstates using ED for small system sizes up to N=18. Since the eigenvalues of $\hat{H}_{\rm eff}$ are complex, the long-time behavior of any initial state is determined by the steady state. Therefore, instead of focusing on eigenstates in the middle of the spectrum, we will report results for the steady state. In particular, the relevant quantities of interest will be the imaginary part of its eigenvalue, which is equal to the steady-state current $[{\rm Im}E_1=J_\infty;\ {\rm see}\ {\rm Eq.}\ (5)],\ {\rm and}\ {\rm the}\ {\rm gap}\ \Delta={\rm Im}E_1-{\rm Im}E_2$ to the first excited state, whose inverse sets the timescale for the approach to the steady state. Notice that we are ordering the eigenvalues from highest to lowest imaginary part.

In general, the determination of extremal eigenvalues of a matrix is a simpler computational task with respect to the full ED of the matrix, or the extraction of eigenvalues in the middle of the spectrum [66,67]. This would suggest that the steady-state properties of the model under consideration could be studied for larger system sizes than the ones usually accessible in the Hermitian counterpart. However, this expectation turns out not to be true for the model under consideration, and one needs to resort to the full ED of the Hamiltonian (see the Supplemental Material [68]).

In Fig. 1, we report the results for the total steady-state current J_{∞} [panel (a)] and the gap Δ to the second largest imaginary eigenvalue [panel (b)]. Our results indicate the absence of a transition at the critical value expected from indicators at the center of the spectrum $h_c \simeq 4.5$ [9,42], marked with a vertical green line in the figure. While the current is indeed suppressed as the disorder strength increases, it always remains finite in the range of parameters studied, going well beyond h_c .

The global current decays as $J_{\infty} \propto e^{-\alpha h}$, with a rate α that depends only weakly on the system size—the precise behavior is hard to determine due to the small range of accessible system sizes. However, one can still confidently see that there is no sign of nonanalyticity in J_{∞} as a function of h. This suggests that no transition occurs in the wide range of disorder strengths explored. These results are consistent with similar observations made in Hermitian models, which also showed exponentially suppressed transport but no signs of nonanalyticity [69,70]. No nonanalyticity is seen even in the dependence of the gap $\Delta \propto e^{-\beta h}$, with a different rate β . Also in this case, the dependence of β on N is too weak to draw any definite conclusion from the small system sizes one has access to.

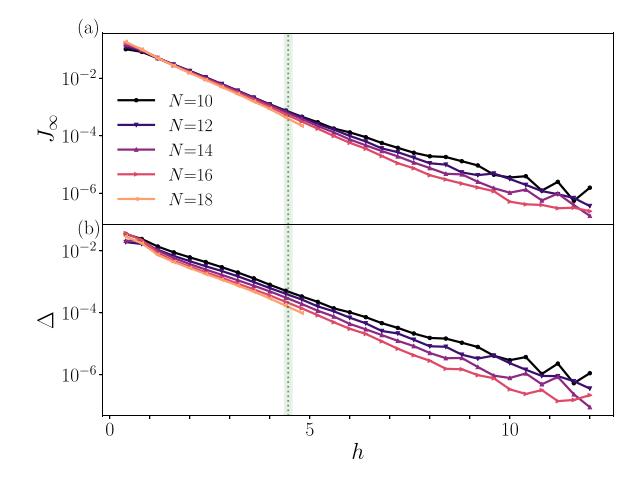


FIG. 1. (a) Steady-state current J_{∞} obtained via exact diagonalization ($N \leqslant 16$) and via time evolution for long times (N=18). Around $h \simeq 4.5$ (green vertical stripe), a non-Hermitian many-body localization transition was previously claimed (see also Fig. 2). However, a weak current persists up to h=12, signaling that the system is actually delocalized. (b) Gap to the first excited state Δ , setting the (inverse) timescale at which the steady state is reached. The data are averaged over 15 000 disorder realizations for $N \leqslant 16$, and over 3000 realizations for N=18.

To better understand why spectral indicators show the presence of an NH MBL transition while no sign is seen in the steady-state current J_{∞} or the gap Δ , we plot the fraction of disorder realizations that yield a completely real spectrum, f_{noSS} , in Fig. 2(a). One can see that the crossover is shifting toward larger values of h. Thus, larger system sizes allow for more delocalized steady states, as also shown by the system size scaling in the inset. The situation is somewhat reminiscent of the drifting of the finite-size critical point in Hermitian systems toward larger disorder values [57,58,71,72].

For comparison, in Fig. 2(b), we show a typical indicator used to detect the NH MBL transition: the average fraction of nonreal eigenvalues in each realization of disorder, $f_{\rm Im}$ [9,42]. Even if $f_{\rm Im}$ displays a crossover around $h_c \simeq 4.5$, and thus in the bulk of the spectrum many eigenvalues become

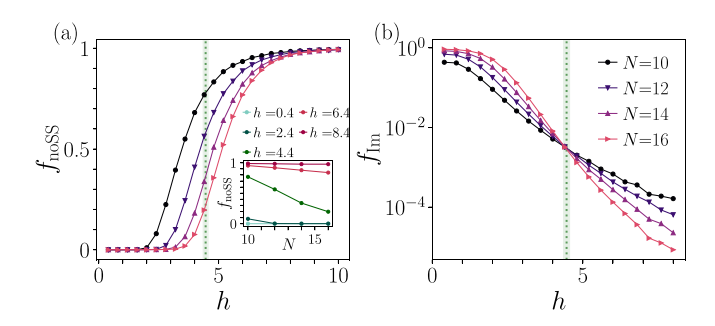


FIG. 2. (a) The fraction $f_{\rm noSS}$ of disorder realizations with a completely real spectrum drifts toward larger values of the disorder strength h, as the system size is increased. Correspondingly, the spectrum becomes more and more delocalized. In the inset, we show the scaling of $f_{\rm noSS}$ with system size at various values of h. (b) Considering instead the average fraction of eigenvalues with a nonzero imaginary part $f_{\rm Im}$, one might conclude that there is an NH MBL transition at the value $h_c \simeq 4.5$ (vertical green stripes). More details are provided in the main text.

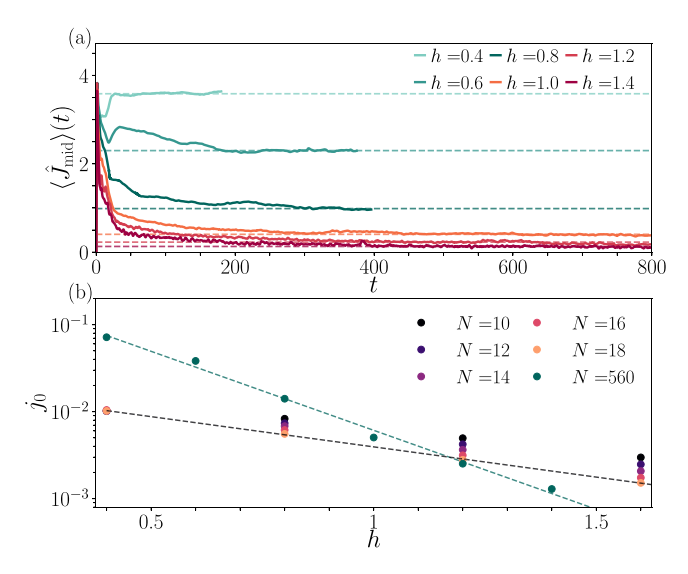


FIG. 3. (a) To avoid boundary effects, we study the current in the central $2\ell_0$ sites of an N=560 chain ($\ell_0=25,35,45$ for increasing disorder). The resulting $\langle \hat{J}_{\text{mid}} \rangle$ shows convergence in time to a plateau $J_0(h)$, before boundary effects eventually kick in. (b) The value J_0 is obtained by averaging the current within a large time window, and we further evaluate the current per site $j_0=J_0/\ell_0$ to be able to compare with exact diagonalization results. The value of j_0 obtained from dynamics also decays exponentially with h, but with a different slope than the one resulting from exact diagonalization.

purely real, the presence of nonzero imaginary eigenvalues well above h_c , testified by $f_{\rm noSS}$, means that at long times the dynamics will be delocalized and with a nonzero current flowing. Other indicators at the center of the spectrum, such as the entanglement entropy or the eigenstate susceptibility, predict a transition at values of h slightly different from 4.5 [42], but all of them consistently show the presence of a bulk transition, which is not reflected in the properties of the steady state

We complement the ED study with simulations of the system's dynamics using matrix product states (MPSs) and an NH version of the time-evolving block decimation algorithm [49]. As MPS algorithms are inefficient in PBCs, we employ OBCs. In OBCs, however, the current is expected to vanish at long times, irrespective of the value of the disorder, as particles accumulate on one of the boundaries (the so-called NH skin effect). To circumvent this issue, we simulate large chains N = 560 and study the dynamics of the current at the center of the chain $\hat{J}_{\text{mid}} = \sum_{j=-\ell_0}^{\ell_0} \hat{J}_{N/2+j}$, where the boundaries affect the system only after a sufficiently long timescale. Based on our ED results under PBCs, we expect a finite current in the bulk before boundary effects kick in. As we show in the Supplemental Material [68], before this timescale, the current dynamics reaches a stable stationary plateau at $J_0(h)$, whose extent increases with system size. We then identify $j_0 = J_0/(2\ell_0)$ as a proxy for the current in the $N \to \infty$ steady state, and we compare it with the ED results, where the other order of limits is taken ($t \to \infty$ first).

In Fig. 3, we report the bulk current dynamics obtained numerically from a Néel initial state $|\psi_0\rangle = |\uparrow\downarrow\uparrow\downarrow\cdots\rangle$ using a large bond dimension $\chi = 768$. The current dynamics [Fig. 3(a)] show a transient effect whose extent depends on

the disorder strength h. At stronger disorder, dynamics are in general slower, leading to a longer transient phenomenon and reaching the plateau later. For the same reason, at weaker disorder boundary effects reach the central part of the chain at earlier times. Nevertheless, at the system size chosen, these timescales allow us to observe the formation of the current plateau, as clearly shown in the figure. As the current dynamics reaches a stationary condition, we use the average over a large time window to extract the value of the plateau J_0 (dashed lines). It is finally important to notice that the current reaches the plateau from above, thus meaning that spin flows (and the system is delocalized) not only asymptotically, but also at intermediate times.

The real-time simulation effectively gives access to values of the current in much larger systems than are reachable by ED. One can then compare these results with the ones presented in Fig. 1(a). In Fig. 3(b), we show the behavior of the intensive bulk current $j_0 = J_0/(2\ell_0)$ and compare it to the ED results, where we take $j_0 = J_{\infty}/N$. Remarkably, the TEBD results confirm the exponential behavior of j_0 as a function of the disorder strength h, at least for small h. This indicates that the exponential scaling observed is robust, and possibly remains valid in the thermodynamic limit also at larger h. Interestingly, the slope of the exponential decay is different between ED and TEBD data. A possible explanation is that the slow drift in the exponent α seen at small system sizes leads to the larger α observed with TEBD. Another explanation could come from the two methods differing dramatically in the order of infinite-time and infinite-system-size limits: While in ED one effectively takes $t \to \infty$ first by analyzing the behavior of eigenstates, in TEBD the opposite is true, as one first takes $N \to \infty$. The possibility of the two limits not commuting highlights yet again how the results on small systems obtained through ED must be interpreted with care [16].

Conclusion. Our study challenges the existence of NH MBL in disordered spin chains by shifting the focus from spectral properties to dynamical transport. Using exact diagonalization and large-scale tensor-network simulations, we demonstrate that the steady-state spin current remains finite at all disorder strengths, decaying exponentially without any nonanalyticity—contrary to expectations from spectral diagnostics. This suggests that the previously identified "crossover" based on midspectrum eigenstates does not manifest in physical observables, raising doubts about the stability of NH MBL in this setting.

Crucially, we find that the limits of infinite time and system size possibly do not commute, with spectral and transport probes yielding quantitatively different conclusions for finite systems. This underscores the necessity of dynamical approaches in studying non-Hermitian systems, where traditional Hermitian paradigms may fail. Our work calls for a reevaluation of NH MBL criteria, emphasizing that localization—if it exists—should be probed through observable quantities like transport, and not just spectral features. These results open new questions about the nature of dissipation-induced phenomena and the robustness of localization in open quantum systems.

Acknowledgments. F.B. thanks Giuseppe de Tomasi and Oskar A. Prośniak for discussion. P.B. acknowledges support by the Austrian Science Fund (FWF) (Grant Agreement

No. 10.55776/ESP9057324). This research was funded in whole or in part by the Austrian Science Fund (FWF) [10.55776/COE1]. The numerical simulations were performed using the ITensor library [73] on the Vienna Scientific Cluster (VSC) and on the MPIPKS HPC cluster. M.L. acknowledges support by the Deutsche Forschungsgemeinschaft (DFG, German Research Foundation) under Germany's

Excellence Strategy—EXC-2111—390814868. F.R. acknowledges support by the European Union-Next Generation EU with the project "Quantum Optics in Many-Body photonic Environments" (QOMBE) code SOE2024 0000084-CUP B77G24000480006.

Data availability. The data that support the findings of this article are openly available [74].

- Z. G. Y. Ashida and M. Ueda, Non-Hermitian physics, Adv. Phys. 69, 249 (2020).
- [2] F. Minganti, A. Miranowicz, R. W. Chhajlany, and F. Nori, Quantum exceptional points of non-Hermitian Hamiltonians and Liouvillians: The effects of quantum jumps, Phys. Rev. A 100, 062131 (2019).
- [3] A. N. Poddubny, Interaction-induced analog of a non-Hermitian skin effect in a lattice two-body problem, Phys. Rev. B 107, 045131 (2023).
- [4] L. Garbe, Y. Minoguchi, J. Huber, and P. Rabl, The bosonic skin effect: Boundary condensation in asymmetric transport, SciPost Phys. 16, 029 (2024).
- [5] J. Gliozzi, G. De Tomasi, and T. L. Hughes, Many-body non-Hermitian skin effect for multipoles, Phys. Rev. Lett. 133, 136503 (2024).
- [6] S. Wang, B. Wang, C. Liu, C. Qin, L. Zhao, W. Liu, S. Longhi, and P. Lu, Nonlinear non-Hermitian skin effect and skin solitons in temporal photonic feedback lattices, Phys. Rev. Lett. 134, 243805 (2025).
- [7] A. Felski and F. K. Kunst, Exceptional points and stability in nonlinear models of population dynamics having PT symmetry, Phys. Rev. Res. 7, 013326 (2025).
- [8] N. H. Kwong, J. Wingenbach, L. Ares, J. Sperling, X. Ma, S. Schumacher, and R. Binder, Universal neighborhood topology and geometry of exceptional points in physical systems, arXiv:2502.19236.
- [9] R. Hamazaki, K. Kawabata, and M. Ueda, Non-Hermitian many-body localization, Phys. Rev. Lett. **123**, 090603 (2019).
- [10] I. V. Gornyi, A. D. Mirlin, and D. G. Polyakov, Interacting electrons in disordered wires: Anderson localization and low-*T* transport, Phys. Rev. Lett. **95**, 206603 (2005).
- [11] D. M. Basko, I. L. Aleiner, and B. L. Altshuler, Metal–insulator transition in a weakly interacting many-electron system with localized single-particle states, Ann. Phys. **321**, 1126 (2006).
- [12] M. Serbyn, Z. Papić, and D. A. Abanin, Local conservation laws and the structure of the many-body localized states, Phys. Rev. Lett. 111, 127201 (2013).
- [13] V. Ros, M. Müller, and A. Scardicchio, Integrals of motion in the many-body localized phase, Nucl. Phys. B **891**, 420 (2015).
- [14] J. Z. Imbrie, Diagonalization and many-body localization for a disordered quantum spin chain, Phys. Rev. Lett. 117, 027201 (2016); On many-body localization for quantum spin chains, J. Stat. Phys. 163, 998 (2016).
- [15] D. A. Abanin, E. Altman, I. Bloch, and M. Serbyn, *Colloquium:* Many-body localization, thermalization, and entanglement, Rev. Mod. Phys. 91, 021001 (2019).
- [16] P. Sierant, M. Lewenstein, A. Scardicchio, L. Vidmar, and J. Zakrzewski, Many-body localization in the age of classical computing, Rep. Prog. Phys. 88, 026502 (2025).

- [17] V. Oganesyan and D. A. Huse, Localization of interacting fermions at high temperature, Phys. Rev. B **75**, 155111 (2007).
- [18] M. Žnidarič, T. Prosen, and P. Prelovšek, Many-body localization in the Heisenberg *XXZ* magnet in a random field, Phys. Rev. B **77**, 064426 (2008).
- [19] A. Pal and D. A. Huse, Many-body localization phase transition, Phys. Rev. B **82**, 174411 (2010).
- [20] A. D. Luca and A. Scardicchio, Ergodicity breaking in a model showing many-body localization, Europhys. Lett. 101, 37003 (2013).
- [21] D. J. Luitz, N. Laflorencie, and F. Alet, Many-body localization edge in the random-field Heisenberg chain, Phys. Rev. B **91**, 081103 (2015).
- [22] R. Nandkishore, S. Gopalakrishnan, and D. A. Huse, Spectral features of a many-body-localized system weakly coupled to a bath, Phys. Rev. B **90**, 064203 (2014).
- [23] S. Gopalakrishnan and R. Nandkishore, Mean-field theory of nearly many-body localized metals, Phys. Rev. B 90, 224203 (2014).
- [24] D. A. Huse, R. Nandkishore, F. Pietracaprina, V. Ros, and A. Scardicchio, Localized systems coupled to small baths: From Anderson to Zeno, Phys. Rev. B 92, 014203 (2015).
- [25] S. Johri, R. Nandkishore, and R. N. Bhatt, Many-body localization in imperfectly isolated quantum systems, Phys. Rev. Lett. 114, 117401 (2015).
- [26] M. H. Fischer, M. Maksymenko, and E. Altman, Dynamics of a many-body-localized system coupled to a bath, Phys. Rev. Lett. 116, 160401 (2016).
- [27] E. Levi, M. Heyl, I. Lesanovsky, and J. P. Garrahan, Robustness of many-body localization in the presence of dissipation, Phys. Rev. Lett. **116**, 237203 (2016).
- [28] M. V. Medvedyeva, T. Prosen, and M. Žnidarič, Influence of dephasing on many-body localization, Phys. Rev. B 93, 094205 (2016)
- [29] R. Nandkishore and S. Gopalakrishnan, Many body localized systems weakly coupled to baths, Ann. Phys. 529, 1600181 (2017).
- [30] D. J. Luitz, F. Huveneers, and W. De Roeck, How a small quantum bath can thermalize long localized chains, Phys. Rev. Lett. **119**, 150602 (2017).
- [31] B. Everest, I. Lesanovsky, J. P. Garrahan, and E. Levi, Role of interactions in a dissipative many-body localized system, Phys. Rev. B 95, 024310 (2017).
- [32] L.-N. Wu, A. Schnell, G. D. Tomasi, M. Heyl, and A. Eckardt, Describing many-body localized systems in thermal environments, New J. Phys. 21, 063026 (2019).
- [33] E. Wybo, M. Knap, and F. Pollmann, Entanglement dynamics of a many-body localized system coupled to a bath, Phys. Rev. B **102**, 064304 (2020).

- [34] P. Brighi, A. A. Michailidis, D. A. Abanin, and M. Serbyn, Propagation of many-body localization in an Anderson insulator, Phys. Rev. B **105**, L220203 (2022).
- [35] N. Hatano and D. R. Nelson, Localization transitions in non-Hermitian quantum mechanics, Phys. Rev. Lett. 77, 570 (1996); Vortex pinning and non-Hermitian quantum mechanics, Phys. Rev. B 56, 8651 (1997); Non-Hermitian delocalization and eigenfunctions, 58, 8384 (1998).
- [36] J. Gliozzi, F. Balducci, T. L. Hughes, and G. D. Tomasi, Non-Hermitian multipole skin effects challenge localization, arXiv:2504.10580.
- [37] L.-J. Zhai, S. Yin, and G.-Y. Huang, Many-body localization in a non-Hermitian quasiperiodic system, Phys. Rev. B 102, 064206 (2020).
- [38] K. Suthar, Y.-C. Wang, Y.-P. Huang, H. H. Jen, and J.-S. You, Non-Hermitian many-body localization with open boundaries, Phys. Rev. B 106, 064208 (2022).
- [39] S. Ghosh, S. Gupta, and M. Kulkarni, Spectral properties of disordered interacting non-Hermitian systems, Phys. Rev. B **106**, 134202 (2022).
- [40] K. Yamamoto and R. Hamazaki, Localization properties in disordered quantum many-body dynamics under continuous measurement, Phys. Rev. B 107, L220201 (2023).
- [41] H.-Z. Li, X.-J. Yu, and J.-X. Zhong, Non-Hermitian Stark many-body localization, Phys. Rev. A 108, 043301 (2023).
- [42] J. Mák, M. J. Bhaseen, and A. Pal, Statics and dynamics of non-Hermitian many-body localization, Commun. Phys. 7, 92 (2024)
- [43] G. De Tomasi and I. M. Khaymovich, Stable many-body localization under random continuous measurements in the no-click limit, Phys. Rev. B 109, 174205 (2024).
- [44] G. Akemann, F. Balducci, A. Chenu, P. Päßler, F. Roccati, and R. Shir, Two transitions in complex eigenvalue statistics: Hermiticity and integrability breaking, Phys. Rev. Res. 7, 013098 (2025).
- [45] F. Roccati, F. Balducci, R. Shir, and A. Chenu, Diagnosing non-Hermitian many-body localization and quantum chaos via singular value decomposition, Phys. Rev. B 109, L140201 (2024).
- [46] P. W. Anderson, Absence of diffusion in certain random lattices, Phys. Rev. 109, 1492 (1958).
- [47] W. D. Roeck, L. Giacomin, F. Huveneers, and O. Prosniak, Absence of normal heat conduction in strongly disordered interacting quantum chains, arXiv:2408.04338.
- [48] A. Panda and S. Banerjee, Entanglement in nonequilibrium steady states and many-body localization breakdown in a current-driven system, Phys. Rev. B **101**, 184201 (2020).
- [49] G. Vidal, Efficient classical simulation of slightly entangled quantum computations, Phys. Rev. Lett. **91**, 147902 (2003).
- [50] S. E. Begg and R. Hanai, Quantum criticality in open quantum spin chains with nonreciprocity, Phys. Rev. Lett. 132, 120401 (2024).
- [51] A. Metelmann and A. A. Clerk, Nonreciprocal photon transmission and amplification via reservoir engineering, Phys. Rev. X 5, 021025 (2015).
- [52] C. C. Wanjura, M. Brunelli, and A. Nunnenkamp, Topological framework for directional amplification in driven-dissipative cavity arrays, Nat. Commun. 11, 3149 (2020).

- [53] D. Porras and S. Fernández-Lorenzo, Topological amplification in photonic lattices, Phys. Rev. Lett. 122, 143901 (2019).
- [54] J. Šuntajs, J. Bonča, T. Prosen, and L. Vidmar, Quantum chaos challenges many-body localization, Phys. Rev. E 102, 062144 (2020).
- [55] R. K. Panda, A. Scardicchio, M. Schulz, S. R. Taylor, and M. Žnidarič, Can we study the many-body localisation transition? Europhys. Lett. 128, 67003 (2020).
- [56] D. Abanin, J. Bardarson, G. De Tomasi, S. Gopalakrishnan, V. Khemani, S. Parameswaran, F. Pollmann, A. Potter, M. Serbyn, and R. Vasseur, Distinguishing localization from chaos: Challenges in finite-size systems, Ann. Phys. 427, 168415 (2021).
- [57] P. J. D. Crowley and A. Chandran, A constructive theory of the numerically accessible many-body localized to thermal crossover, SciPost Phys. 12, 201 (2022).
- [58] A. Morningstar, L. Colmenarez, V. Khemani, D. J. Luitz, and D. A. Huse, Avalanches and many-body resonances in many-body localized systems, Phys. Rev. B 105, 174205 (2022).
- [59] P. J. D. Crowley and A. Chandran, Mean-field theory of failed thermalizing avalanches, Phys. Rev. B 106, 184208 (2022).
- [60] D. M. Long, P. J. D. Crowley, V. Khemani, and A. Chandran, Phenomenology of the prethermal many-body localized regime, Phys. Rev. Lett. 131, 106301 (2023).
- [61] Due to our conventions of *i*'s, the states with positive imaginary eigenenergies are amplified, while those with negative imaginary eigenenergies are suppressed.
- [62] K. Kawabata, T. Numasawa, and S. Ryu, Entanglement phase transition induced by the non-Hermitian skin effect, Phys. Rev. X 13, 021007 (2023).
- [63] D. E. Mahoney and J. Richter, Transport and integrabilitybreaking in non-Hermitian many-body quantum systems, Phys. Rev. B 110, 134302 (2024).
- [64] M. Naghiloo, M. Abbasi, Y. N. Joglekar, and K. W. Murch, Quantum state tomography across the exceptional point in a single dissipative qubit, Nat. Phys. 15, 1232 (2019).
- [65] J. Cuerda, J. M. Taskinen, N. Källman, L. Grabitz, and P. Törmä, Observation of quantum metric and non-Hermitian Berry curvature in a plasmonic lattice, Phys. Rev. Res. 6, L022020 (2024).
- [66] F. Pietracaprina, N. Macé, D. J. Luitz, and F. Alet, Shift-invert diagonalization of large many-body localizing spin chains, SciPost Phys. 5, 045 (2018).
- [67] P. Sierant, M. Lewenstein, and J. Zakrzewski, Polynomially filtered exact diagonalization approach to many-body localization, Phys. Rev. Lett. 125, 156601 (2020).
- [68] See Supplemental Material at http://link.aps.org/supplemental/ 10.1103/crwj-x7j8 for additional information on the numerical procedures.
- [69] V. Oganesyan, A. Pal, and D. A. Huse, Energy transport in disordered classical spin chains, Phys. Rev. B 80, 115104 (2009).
- [70] M. Žnidarič and M. Ljubotina, Interaction instability of localization in quasiperiodic systems, Proc. Natl. Acad. Sci. USA 115, 4595 (2018).
- [71] T. Scoquart, I. V. Gornyi, and A. D. Mirlin, Role of Fock-space correlations in many-body localization, Phys. Rev. B 109, 214203 (2024).

- [72] J. Niedda, G. B. Testasecca, G. Magnifico, F. Balducci, C. Vanoni, and A. Scardicchio, Renormalization-group analysis of the many-body localization transition in the random-field XXZ chain, Phys. Rev. B 112, 144201 (2025).
- [73] M. Fishman, S. R. White, and E. M. Stoudenmire, The ITensor software library for tensor network calculations, SciPost Phys. Codebases 4 (2022).
- [74] Visit http://doi.org/10.5281/zenodo.17118846 for all the data necessary to reproduce figures.